

Electronic Supplementary Material (ESI) for Inorganic Chemistry Frontiers.
This journal is © the Partner Organisations 2024

Supporting Information

Cation and Anion Co-Partial Substitution Induced Centrosymmetric to Noncentrosymmetric Structural Transformation to Construct Nonlinear-Optical Rare-Earth Oxythiogermanates

Nan Zhang,^a Mei Yang,^a Wen-Dong Yao,^a Wei Xu,^a Wenfeng Zhou,^a Wenlong Liu,^a and Sheng-Ping Guo^{a,b*}

^aSchool of Chemistry & Chemical Engineering, Yangzhou University, Yangzhou, Jiangsu 22500

^bYunnan Key Laboratory of Electromagnetic Materials and Devices, National Center for International Research on Photoelectric and Energy Materials, School of Materials and Energy, Yunnan University, Kunming, Yunnan 650091

*Corresponding author: spguo@yzu.edu.cn; spguo@ynu.edu.cn

Contents

1. Tables

Table S1. Crystal data and structure refinement parameters for **1–3**.

Table S2. Atomic coordinates ($\times 10^4$) and equivalent isotropic displacement parameters (U_{eq}^{a} , $\text{\AA}^2 \times 10^3$) for **1–3**.

Table S3. Bond distances for **1–3**.

Table S4. LIDTs of **1**, **2** and AGS for their powder samples (75–110 μm).

Table S5. Thermal expansion coefficients (TECs, αL) ($\times 10^{-5} \text{K}^{-1}$) of **1**, **2** and the reference AGS along *a*-, *b*- and *c*-axis, and the thermal expansion anisotropy (TEA, δ) of **1**, **2** and AGS.

Table S6. NLO properties of **1–3** and other reported rare-earth oxychalcogenides.

Table S7. The calculated dipole moments (esu cm \AA^{-3}) in one unit cell of **1** and **2**.

Table S8. Distortion degrees of polyhedral units in **1** and **2**.

2. Figures

Figure S1. The crystals' photographs of **1–3**.

Figure S2. The powder XRD patterns of **1–3**.

Figure S3. The EDS images for single crystals of **1–3**.

Figure S4. Coordination geometry of **0**.

Figure S5. Coordination geometries of **1–3**.

Figure S6. Photographs of **1–3** for the measurements of birefringence with polarizing microscope.

Figure S7. DSC curves of **1** and **2**.

Figure S8. The powder XRD patterns of **1** and **2** after calcination.

Figure S9. The calculated SHG tensors and birefringences of **1–3**.

Figure S10. The calculated dipole moments for one unit cell of **1** and **2**.

3. References

1. Tables

Table S1. Crystal data and structure refinement parameters for 1–3.

Chemical formula	Eu ₁₈ Ge ₉ O ₅ S ₃₁ (1)	Ca _{3.32} Eu _{14.68} Ge ₉ O ₅ S ₃₁ (2)	Ba ₃ Eu ₁₅ Ge ₉ O ₅ S ₃₁ (3)
Formula weight	4462.45	4091.01	4418.59
Temperature (K)		296	
Crystal system		trigonal	
Space group		<i>R</i> 3	
<i>a</i> (Å)	16.8496(4)	16.7573(8)	16.8834(7)
<i>c</i> (Å)	17.9927(6)	17.9107(9)	18.0091(8)
γ /°		120	
<i>V</i> (Å ³)	4423.9(3)	4355.6(5)	4445.7(4)
<i>Z</i>		3	
<i>D</i> _{calc} (g/cm ³)	5.025	4.679	4.951
μ (mm ⁻¹)	24.431	21.588	23.148
<i>F</i> (000)	5874.0	5446.0	5811.0
2 θ range (°)	4.836 to 56.706	4.862 to 61.032	3.588 to 50.036
Indep. reflns/ <i>R</i> _{int}	4356/0.0319	5845/0.0438	3514/0.0379
GOF on <i>F</i> ²	0.974	1.047	1.187
Flack parameter	-0.001(9)	-0.009(8)	0.09(3)
<i>R</i> 1 ^a , <i>wR</i> 2 ^b [<i>I</i> ≥ 2 σ (<i>I</i>)]	0.0189, 0.0310	0.0265, 0.0510	0.0283, 0.0693
<i>R</i> 1 ^a , <i>wR</i> 2 ^b [all data]	0.0207, 0.0314	0.0291, 0.0516	0.0291, 0.0701
Largest diff. peak/hole/e Å ⁻³	0.84/-0.90	0.96/-2.39	2.29/-2.55

$${}^a\text{R1} = \frac{\sum ||F_o| - |F_c||}{\sum |F_o|}; \quad {}^b\text{wR2} = \left\{ \frac{[\sum w(F_o^2 - F_c^2)^2]}{[\sum w(F_o^2)^2]} \right\}^{1/2}.$$

Table S2. Atomic coordinates ($\times 10^4$) and equivalent isotropic displacement parameters (U_{eq}^a , $\text{\AA}^2 \times 10^3$) for **1–3**.

Atom	Wyck. site	Occupancy	x	y	z	U_{eq}
1						
Eu(1)	<i>9b</i>	1	1341.3(3)	8239.2(3)	6710.7(2)	11.68(9)
Eu(2)	<i>9b</i>	1	3254.2(3)	8055.3(3)	8051.4(2)	12.18(9)
Eu(3)	<i>9b</i>	1	1283.1(3)	9902.3(3)	4854.7(2)	10.29(9)
Eu(4)	<i>9b</i>	1	-1467.2(3)	6728.5(3)	6671.2(2)	11.32(9)
Eu(5)	<i>9b</i>	1	1784.6(3)	6679.1(3)	5234.8(2)	12.00(9)
Eu(6)	<i>9b</i>	1	1773.0(3)	8325.7(3)	9993.8(2)	10.91(9)
Ge(1)	<i>3a</i>	1	0	10000	3359.5(7)	7.1(3)
Ge(2)	<i>3a</i>	1	3333.33	6666.67	3243.9(7)	7.9(3)
Ge(3)	<i>9b</i>	1	3263.6(5)	9828.1(5)	5416.3(4)	6.78(17)
Ge(4)	<i>9b</i>	1	4.1(5)	6540.1(5)	7972.5(4)	6.17(17)
Ge(5)	<i>3a</i>	1	3333.33	6666.67	6720.4(8)	6.9(3)
S(1)	<i>3a</i>	1	3333.33	6666.67	4469.4(17)	13.4(7)
S(2)	<i>9b</i>	1	3312.8(12)	7899.5(12)	6330.8(10)	11.2(4)
S(3)	<i>9b</i>	1	3167.4(12)	9934.1(12)	6640.3(9)	10.0(4)
S(4)	<i>9b</i>	1	-1261.0(12)	5327.1(13)	7573.9(10)	9.1(4)
S(5)	<i>9b</i>	1	1993.7(12)	8803.8(13)	8385.8(10)	9.5(4)
S(6)	<i>9b</i>	1	1253.7(12)	6581.7(12)	7521.5(10)	9.9(4)
S(7)	<i>9b</i>	1	3295.0(13)	11084.1(12)	5015.5(9)	9.6(4)
S(8)	<i>9b</i>	1	3414.6(13)	7979.9(13)	9713.5(11)	12.5(4)

S(9)	9b	1	2017.3(12)	8604.1(12)	5041.7(10)	10.3(4)
S(10)	9b	1	99.5(13)	6786.6(13)	9183.3(10)	9.0(4)
S(11)	9b	1	-68.6(13)	8757.3(12)	6102.3(10)	11.7(4)
O(1)	3a	1	0	10000	4354(4)	8.7(18)
O(2)	3a	1	3333.33	6666.67	7724(4)	6.6(17)
O(3)	9b	1	-19(3)	7482(3)	7535(2)	8.3(10)

2

Eu(1)	9b	0.848	1353.5(3)	8243.4(4)	6712.0(3)	13.59(15)
Eu(2)	9b	0.750	3261.8(4)	8058.7(4)	8049.9(3)	12.97(18)
Eu(3)	9b	0.762	1283.4(4)	9905.5(4)	4848.1(3)	11.18(17)
Eu(4)	9b	1	-1466.3(3)	6734.7(3)	6668.5(2)	12.33(12)
Eu(5)	9b	0.705	1787.8(4)	6678.4(4)	5232.8(4)	13.28(19)
Eu(6)	9b	0.829	1767.3(4)	8329.2(4)	9994.7(3)	11.76(15)
Ca(1)	9b	0.152	1353.5(3)	8243.4(4)	6712.0(3)	13.59(15)
Ca(2)	9b	0.250	3261.8(4)	8058.7(4)	8049.9(3)	12.97(18)
Ca(3)	9b	0.238	1283.4(4)	9905.5(4)	4848.1(3)	11.18(17)
Ca(5)	9b	0.295	1787.8(4)	6678.4(4)	5232.8(4)	13.28(19)
Ca(6)	9b	0.171	1767.3(4)	8329.2(4)	9994.7(3)	11.76(15)
Ge(1)	9b	1	0	10000	3358.0(8)	7.4(3)
Ge(2)	9b	1	3333.33	6666.67	3250.5(8)	8.6(3)
Ge(3)	3a	1	3264.0(6)	9832.0(6)	5419.9(5)	7.71(19)
Ge(4)	3a	1	7.6(6)	6548.8(6)	7976.7(5)	6.60(18)
Ge(5)	3a	1	3333.33	6666.67	6723.8(9)	8.4(3)

S(1)	9b	1	3333.33	6666.67	4475(2)	18.1(8)
S(2)	9b	1	3309.7(15)	7903.7(14)	6330.3(12)	13.5(4)
S(3)	9b	1	3168.8(15)	9931.7(14)	6649.5(12)	12.7(4)
S(4)	9b	1	-1258.8(14)	5330.2(14)	7567.7(11)	8.8(4)
S(5)	9b	1	1997.6(14)	8795.7(14)	8389.8(11)	10.9(4)
S(6)	9b	1	1258.7(14)	6584.4(14)	7523.0(12)	10.9(4)
S(7)	9b	1	3288.8(15)	11088.4(14)	5015.8(11)	11.6(4)
S(8)	9b	1	3410.1(14)	7980.1(14)	9706.7(12)	12.6(4)
S(9)	9b	1	2007.8(13)	8604.1(14)	5043.1(12)	11.3(4)
S(10)	9b	1	94.6(14)	6795.3(14)	9191.1(11)	9.3(4)
S(11)	9b	1	-59.2(15)	8761.2(14)	6097.0(12)	13.6(4)
O(1)	9b	1	0	10000	4352(5)	8(2)
O(2)	3a	1	3333.33	6666.67	7740(5)	10(2)
O(3)	3a	1	-7(4)	7506(4)	7536(3)	8.5(11)
3						
Ba(1)	9b	1	8452.5(7)	8443.2(7)	5309.7(7)	5.5(3)
Eu(1)	9b	1	6886.4(8)	8237.3(7)	3453.6(5)	14.3(3)
Eu(2)	9b	1	4797.7(7)	8053.9(7)	4798.4(6)	13.6(3)
Eu(3)	9b	1	8196.7(8)	6726.6(9)	3413.7(6)	13.6(3)
Eu(4)	9b	1	7953.0(7)	4714.7(7)	4928.6(6)	12.0(3)
Eu(5)	9b	1	9893.0(7)	4986.4(8)	3406.3(6)	13.5(3)
Ge(1)	3a	1	3333.33	6666.67	6776.6(19)	7.0(7)
Ge(2)	3a	1	10000	10000	3329(2)	9.1(8)

Ge(3)	<i>9b</i>	1	6541.8(14)	6547.2(14)	4721.4(12)	6.3(4)
Ge(4)	<i>9b</i>	1	9933.0(14)	6769.5(14)	5494.1(12)	9.3(5)
Ge(5)	<i>3a</i>	1	10000	10000	6804(2)	7.0(7)
S(1)	<i>3a</i>	1	10000	10000	4542(5)	15.7(18)
S(2)	<i>9b</i>	1	6584(3)	5330(3)	4323(3)	10.6(10)
S(3)	<i>9b</i>	1	3419(3)	8748(3)	4274(3)	11.1(10)
S(4)	<i>9b</i>	1	8824(3)	8767(4)	2845(3)	15.8(11)
S(5)	<i>9b</i>	1	9980(3)	8748(3)	6411(3)	11.7(10)
S(6)	<i>9b</i>	1	8683(3)	6744(3)	5121(3)	12.0(10)
S(7)	<i>9b</i>	1	9960(3)	5545(3)	5088(3)	11.4(10)
S(8)	<i>9b</i>	1	4570(3)	7968(3)	6454(3)	13.5(10)
S(9)	<i>9b</i>	1	6807(3)	8806(3)	5128(3)	11.4(10)
S(10)	<i>9b</i>	1	6696(3)	6790(3)	5927(3)	9.5(10)
S(11)	<i>9b</i>	1	9843(3)	6584(3)	6718(3)	12.2(10)
O(1)	<i>9b</i>	1	7508(10)	7502(9)	4272(7)	13(3)
O(2)	<i>3a</i>	1	3333.33	6666.67	7778(12)	7.8(18)
O(3)	<i>3a</i>	1	10000	10000	7823(12)	9(5)

^a U_{eq} is defined as 1/3 of the trace of the orthogonalized U_{ij} tensor.

Table S3. Bond distances for **1–3**.

Bond	Distance/Å	Bond	Distance/Å
1			
Eu(1)–S(3)	2.9752(18)	Eu(5)–S(5) ²	3.1358(18)
Eu(1)–S(5)	3.1863(18)	Eu(5)–S(9)	3.0860(19)
Eu(1)–S(6)	3.0883(19)	Eu(5)–S(10) ²	3.088(19)
Eu(1)–S(9)	3.1611(19)	Eu(5)–O(3) ²	2.457(5)
Eu(1)–S(10) ²	3.0031(19)	Eu(6)–S(2) ⁶	3.4314(19)
Eu(1)–S(11)	3.1110(19)	Eu(6)–S(3) ⁶	2.961(19)
Eu(1)–O(3)	2.482(4)	Eu(6)–S(4) ¹	2.8952(18)
Eu(2)–S(2)	3.1127(18)	Eu(6)–S(5)	2.9763(18)
Eu(2)–S(5)	3.0237(18)	Eu(6)–S(6) ¹	3.0407(18)
Eu(2)–S(6) ³	3.2258(19)	Eu(6)–S(7) ¹²	3.1607(17)
Eu(2)–S(6)	3.1729(19)	Eu(6)–S(8)	3.1397(19)
Eu(2)–S(7) ⁶	2.9640(19)	Eu(6)–S(10)	3.0807(19)
Eu(2)–S(8)	3.011(2)	Ge(1)–S(8) ¹³	2.2200(19)
Eu(2)–O(2)	2.4803(18)	Ge(1)–S(8) ¹⁴	2.2200(18)
Eu(3)–S(4) ²	3.1498(18)	Ge(1)–S(8) ⁹	2.2199(19)
Eu(3)–S(4) ¹⁰	3.2744(18)	Ge(1)–O(1)	1.789(7)
Eu(3)–S(7)	2.9649(19)	Ge(2)–S(1)	2.205(3)
Eu(3)–S(8) ⁹	3.254(2)	Ge(2)–S(11) ²	2.2104(19)
Eu(3)–S(9)	3.0223(19)	Ge(2)–S(11) ¹⁵	2.2106(19)
Eu(3)–S(11)	3.091(19)	Ge(2)–S(11) ⁵	2.2105(19)
Eu(3)–S(11) ⁸	3.1276(19)	Ge(3)–S(3)	2.2219(19)

Eu(3)–O(1)	2.423(3)	Ge(3)–S(5) ⁵	2.2089(19)
Eu(4)–S(3) ⁷	3.0679(18)	Ge(3)–S(7)	2.2112(19)
Eu(4)–S(4)	3.0256(18)	Ge(3)–S(9)	2.1878(19)
Eu(4)–S(7) ⁷	3.2246(17)	Ge(4)–S(4)	2.209(2)
Eu(4)–S(8) ¹¹	3.328(19)	Ge(4)–S(6)	2.225(2)
Eu(4)–S(9) ¹	3.1704(19)	Ge(4)–S(10)	2.2086(19)
Eu(4)–S(10) ²	3.0367(19)	Ge(4)–O(3)	1.789(5)
Eu(4)–S(11)	3.1986(19)	Ge(5)–S(2) ³	2.2090(19)
Eu(4)–O(3)	2.623(5)	Ge(5)–S(2)	2.2089(19)
Eu(5)–S(1)	2.9600(15)	Ge(5)–S(2) ⁴	2.2089(19)
Eu(5)–S(2) ⁴	3.1395(19)	Ge(5)–O(2)	1.806(8)
Eu(5)–S(2)	3.0745(19)		

2

Eu(1)/Ca(1)–S(3)	2.943(2)	Eu(5)/Ca(5)–S(5) ¹	3.130(2)
Eu(1)/Ca(1)–S(5)	3.171(2)	Eu(5)/Ca(5)–S(9)	3.078(2)
Eu(1)/Ca(1)–S(6)	3.070(2)	Eu(5)/Ca(5)–S(10) ¹	3.066(2)
Eu(1)/Ca(1)–S(9)	3.137(2)	Eu(5)/Ca(5)–O(3) ¹	2.425(6)
Eu(1)/Ca(1)–S(10) ¹	2.980(2)	Eu(6)/Ca(6)–S(2) ²	3.398(2)
Eu(1)/Ca(1)–S(11)	3.102(2)	Eu(6)/Ca(6)–S(3) ²	2.941(2)
Eu(1)/Ca(1)–O(3)	2.467(5)	Eu(6)/Ca(6)–S(4) ⁷	2.880(2)
Eu(2)/Ca(2)–S(2)	3.095(2)	Eu(6)/Ca(6)–S(5)	2.953(2)
Eu(2)/Ca(2)–S(5)	3.000(2)	Eu(6)/Ca(6)–S(6) ⁷	3.021(2)
Eu(2)/Ca(2)–S(6)	3.157(2)	Eu(6)/Ca(6)–S(7) ¹¹	3.141(2)
Eu(2)/Ca(2)–S(6) ³	3.194(2)	Eu(6)/Ca(6)–S(8)	3.130(2)

Eu(2)/Ca(2)–S(7) ²	2.953(2)	Eu(6)/Ca(6)–S(10)	3.055(2)
Eu(2)/Ca(2)–S(8)	2.986(2)	Ge(1)–S(8) ⁵	2.214(2)
Eu(2)/Ca(2)–O(2)	2.458(2)	Ge(1)–S(8) ¹²	2.214(2)
Eu(3)/Ca(3)–S(4) ¹	3.139(2)	Ge(1)–S(8) ¹³	2.214(2)
Eu(3)/Ca(3)–S(4) ⁴	3.256(2)	Ge(1)–O(1)	1.781(9)
Eu(3)/Ca(3)–S(7)	2.941(2)	Ge(2)–S(1)	2.194(4)
Eu(3)/Ca(3)–S(8) ⁵	3.240(2)	Ge(2)–S(11) ¹⁴	2.208(2)
Eu(3)/Ca(3)–S(9)	3.000(2)	Ge(2)–S(11) ¹⁵	2.208(2)
Eu(3)/Ca(3)–S(11)	3.070(2)	Ge(2)–S(11) ¹	2.208(2)
Eu(3)/Ca(3)–S(11) ⁶	3.119(2)	Ge(3)–S(3)	2.220(2)
Eu(3)/Ca(3)–O(1)	2.404(3)	Ge(3)–S(5) ¹⁴	2.203(2)
Eu(4)–S(3) ⁸	3.051(2)	Ge(3)–S(7)	2.207(2)
Eu(4)–S(4)	3.012(2)	Ge(3)–S(9)	2.188(2)
Eu(4)–S(7) ⁸	3.198(2)	Ge(4)–S(4)	2.208(2)
Eu(4)–S(8) ⁹	3.320(2)	Ge(4)–S(6)	2.221(2)
Eu(4)–S(9) ⁷	3.160(2)	Ge(4)–S(10)	2.205(2)
Eu(4)–S(10) ¹	3.031(2)	Ge(4)–O(3)	1.798(6)
Eu(4)–S(11)	3.183(2)	Ge(5)–S(2) ¹⁰	2.208(2)
Eu(4)–O(3)	2.627(5)	Ge(5)–S(2) ³	2.208(2)
Eu(5)/Ca(5)–S(1)	2.9324(18)	Ge(5)–S(2)	2.208(2)
Eu(5)/Ca(5)–S(2)	3.057(2)	Ge(5)–O(2)	1.820(10)
Eu(5)/Ca(5)–S(2) ¹⁰	3.127(2)		
		3	
Ba(1)–S(1)	2.963(4)	Eu(4)–S(6)	3.026(5)

Ba(1)–S(5) ¹	3.145(5)	Eu(4)–S(7)	2.963(5)
Ba(1)–S(5)	3.086(5)	Eu(4)–S(8) ¹⁰	3.258(5)
Ba(1)–S(6)	3.101(5)	Eu(4)–O(2) ¹⁰	2.419(8)
Ba(1)–S(9)	3.147(5)	Eu(5)–S(2) ¹²	2.894(5)
Ba(1)–S(10)	3.089(5)	Eu(5)–S(3) ²	3.035(5)
Ba(1)–O(1)	2.455(14)	Eu(5)–S(5) ⁹	3.433(5)
Eu(1)–S(3) ⁶	3.093(5)	Eu(5)–S(7)	3.157(5)
Eu(1)–S(4)	3.127(5)	Eu(5)–S(8) ¹⁰	3.148(5)
Eu(1)–S(6) ⁵	3.154(5)	Eu(5)–S(9) ¹⁰	2.988(5)
Eu(1)–S(9)	3.188(5)	Eu(5)–S(10) ¹⁰	3.076(5)
Eu(1)–S(10) ⁵	3.000(5)	Eu(5)–S(11) ⁹	2.962(5)
Eu(1)–S(11) ⁵	2.975(5)	Ge(1)–S(8) ⁷	2.222(5)
Eu(1)–O(1)	2.473(13)	Ge(1)–S(8) ⁶	2.222(5)
Eu(2)–S(3)	3.226(5)	Ge(1)–S(8)	2.222(5)
Eu(2)–S(3) ⁶	3.179(5)	Ge(1)–O(2)	1.80(2)
Eu(2)–S(5) ⁵	3.116(5)	Ge(2)–S(1)	2.184(9)
Eu(2)–S(7) ¹	2.971(5)	Ge(2)–S(4) ¹	2.213(5)
Eu(2)–S(8)	3.001(5)	Ge(2)–S(4)	2.213(5)
Eu(2)–S(9)	3.028(5)	Ge(2)–S(4) ²	2.213(5)
Eu(2)–O(3) ⁸	2.473(5)	Ge(3)–S(2)	2.212(5)
Eu(3)–S(2)	3.039(5)	Ge(3)–S(3) ⁶	2.229(5)
Eu(3)–S(4)	3.224(5)	Ge(3)–S(10)	2.202(5)
Eu(3)–S(6)	3.179(5)	Ge(3)–O(1)	1.813(14)
Eu(3)–S(7) ⁹	3.234(5)	Ge(4)–S(6)	2.194(5)

Eu(3)–S(8) ¹⁰	3.353(5)	Ge(4)–S(7)	2.215(5)
Eu(3)–S(10) ⁵	3.052(5)	Ge(4)–S(9) ²	2.205(5)
Eu(3)–S(11) ⁹	3.092(5)	Ge(4)–S(11)	2.220(5)
Eu(3)–O(1)	2.641(13)	Ge(5)–S(5) ²	2.214(5)
Eu(4)–S(2) ¹²	3.274(5)	Ge(5)–S(5) ¹	2.214(5)
Eu(4)–S(2)	3.163(5)	Ge(5)–S(5)	2.214(5)
Eu(4)–S(4) ¹³	3.142(5)	Ge(5)–O(3)	1.830(2)
Eu(4)–S(4) ³	3.089(5)		

Symmetry transformation used to generate equivalent atoms: **1:** ¹2/3-y, 4/3+x-y, 1/3+z; ²-2/3+y-x, 2/3-x, -1/3+z; ³+y-x, 1-x, +z; ⁴1-y, 1+x-y, +z; ⁵4/3-y, 5/3+x-y, -1/3+z; ⁶-1/3+y-x, 4/3-x, 1/3+z; ⁷-1+y-x, 1-x,+z; ⁸1-y, 2+x-y, +z; ⁹-1/3+y-x, 4/3-x, -2/3+z; ¹⁰1/3+x, 2/3+y, -1/3+z; ¹¹-2/3+x, -1/3+y, -1/3+z; ¹²4/3-y, 5/3+x-y, 2/3+z; ¹³2/3-y, 4/3+x-y, -2/3+z; ¹⁴-1/3+x, 1/3+y, -2/3+z; ¹⁵1/3+x, -1/3+y, -1/3+z. **2:** ¹-2/3+y-x, 2/3-x, -1/3+z; ²-1/3+y-x, 4/3-x, 1/3+z; ³+y-x, 1-x, +z; ⁴1/3+x, 2/3+y, -1/3+z; ⁵-1/3+y-x, 4/3-x, -2/3+z; ⁶1-y, 2+x-y, +z; ⁷2/3-y, 4/3+x-y, 1/3+z; ⁸-1+y-x, 1-x, +z; ⁹-2/3+x, -1/3+y, -1/3+z; ¹⁰1-y, 1+x-y, +z; ¹¹4/3-y, 5/3+x-y, 2/3+z; ¹²-1/3+x, 1/3+y, -2/3+z; ¹³2/3-y, 4/3+x-y, -2/3+z; ¹⁴4/3-y, 5/3+x-y, -1/3+z; ¹⁵1/3+x, -1/3+y, -1/3+z. **3:** ¹1+y-x, 2-x, +z; ²2-y, 1+x-y, +z; ³2/3+y-x, 4/3-x, 1/3+z; ⁴-1/3+x, 1/3+y, 1/3+z; ⁵4/3-y, 2/3+x-y, -1/3+z; ⁶+y-x, 1-x, +z; ⁷1-y, 1+x-y, +z; ⁸-2/3+x, -1/3+y, -1/3+z; ⁹4/3+y-x, 5/3-x, -1/3+z; ¹⁰1/3+x, -1/3+y, -1/3+z; ¹¹1-y, +x-y, +z; ¹²1+y-x, 1-x, +z; ¹³5/3-y, 1/3+x-y, 1/3+z.

Table S4. LIDTs of **1**, **2** and AGS for their powder samples (75–110 μm).

Compound	Damage energy (mJ)	Spot area (cm^2)	Damage threshold (MW/cm^2)	Relative value
1	2.3	0.02	11.44	3.3
2	2.3	0.02	11.44	3.3
AGS	0.6	0.02	3.48	1

Table S5. Thermal expansion coefficients (TECs, α_L) ($\times 10^{-5} \text{K}^{-1}$) of **1**, **2** and the reference AGS along *a*-, *b*- and *c*-axis, and the thermal expansion anisotropy (TEA, δ) of **1**, **2** and AGS.

Compound	<i>a</i> [10^{-5}K^{-1}]	<i>b</i> [10^{-5}K^{-1}]	<i>c</i> [10^{-5}K^{-1}]	δ
1	-1.58	-1.58	-4.08	2.58
2	1.49	1.49	0.77	1.94
AGS	3.08	3.08	-9.158	2.97

Table S6. NLO properties of 1–3 and other reported rare-earth oxychalcogenides.

Compound	Space group	E_g (eV)	SHG (\times AGS)	LIDT (\times AGS)	Δn	PM/NPM	Reference
Sm ₃ NbO ₄ S ₃	<i>Pna2</i> ₁	2.68	0.3	12.5	-	PM	1
Gd ₃ NbO ₄ S ₃	<i>Pna2</i> ₁	2.74	0.4	4.5	-	PM	1
La ₃ Ga ₃ Ge ₂ O ₁₀ S ₃	$\bar{P}6$ ₂ <i>c</i>	4.7	2 KDP	-	0.11	PM	2
LaCaGa ₃ OS ₆	$\bar{P}4$ ₂ <i>m</i>	3.27	0.9	14.0	0.163	PM	3
LaSrGa ₃ OS ₆	$\bar{P}4$ ₂ <i>m</i>	3.21	1.0	14.0	0.138	PM	3
Eu ₃ GeOS ₄	<i>Pca2</i> ₁	2.05	0.24	8.86	0.019	NPM	4
Nd ₃ [Ga ₃ O ₃ S ₃][Ge ₂ O ₇]	$\bar{P}6$ ₂ <i>c</i>	4.35	0.8	23.0	0.091	PM	5
Eu ₂ MnGe ₂ OS ₆	$\bar{P}4$ ₂ <i>m</i>	2.40	0.3	8.3	0.13	PM	6
Eu ₂ FeGe ₂ OS ₆	$\bar{P}4$ ₂ <i>m</i>	2.11	0.3	2.8	0.12	PM	6
Eu ₂ CoGe ₂ OS ₆	$\bar{P}4$ ₂ <i>m</i>	2.14	0.5	3.2	0.17	PM	6
Eu ₁₈ Ge ₉ O ₅ S ₃₁	<i>R3</i>	2.18	0.5	3.3	0.0749	PM	this work
Ca _{3.32} Eu _{14.68} Ge ₉ O ₅ S ₃₁	<i>R3</i>	2.23	0.6	3.3	0.0543	PM	this work
Ba ₃ Eu ₁₅ Ge ₉ O ₅ S ₃₁	<i>R3</i>	2.24	-	-	0.0282	-	this work

“-” indicates no available data.

PM: phase-matchable; NPM: non-phase-matchable.

Table S7. The calculated dipole moments (esu cm Å⁻³) in one unit cell of **1** and **2**.

Structural unit	GeS ₄	GeOS ₃	Total
1			
Dipole moment (esu cm Å ⁻³)	0.085	0.116	0.201
2			
Dipole moment (esu cm Å ⁻³)	0.096	0.120	0.216

Table S8. Distortion degrees of polyhedral units in **1** and **2**.

Unite	DI (M-S/O)	DI (S-M-S/O)	DI (S-S/O)
1			
Ge(1)OS ₃	0.076503	0.04179	0.96841
Ge(2)S ₄	0.000917	0.03069	0.96704
Ge(3)S ₄	0.004062	0.02791	0.96708
Ge(4)OS ₃	0.072664	0.03683	0.96841
Ge(5)OS ₃	0.071673	0.00882	0.9696
2			
Ge(1)OS ₃	0.07711	0.03986	0.9685
Ge(2)S ₄	0.002381	0.03582	0.96713
Ge(3)S ₄	0.004083	0.02714	0.96712
Ge(4)OS ₃	0.073529	0.03711	0.96848
Ge(5)OS ₃	0.068925	0.00777	0.96846

Distortion degree: the average deviation of bond lengths, bond angles and side lengths from their means.

2. Figures

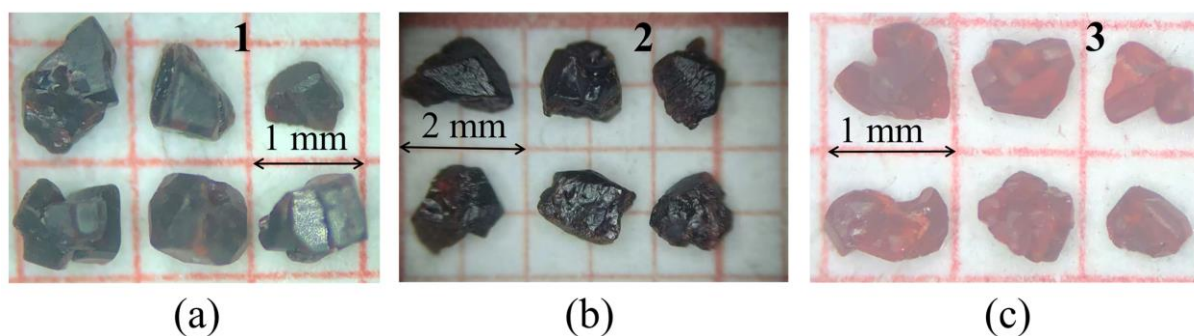


Figure S1. The crystals' photographs of **1** (a), **2** (b) and **3** (c).

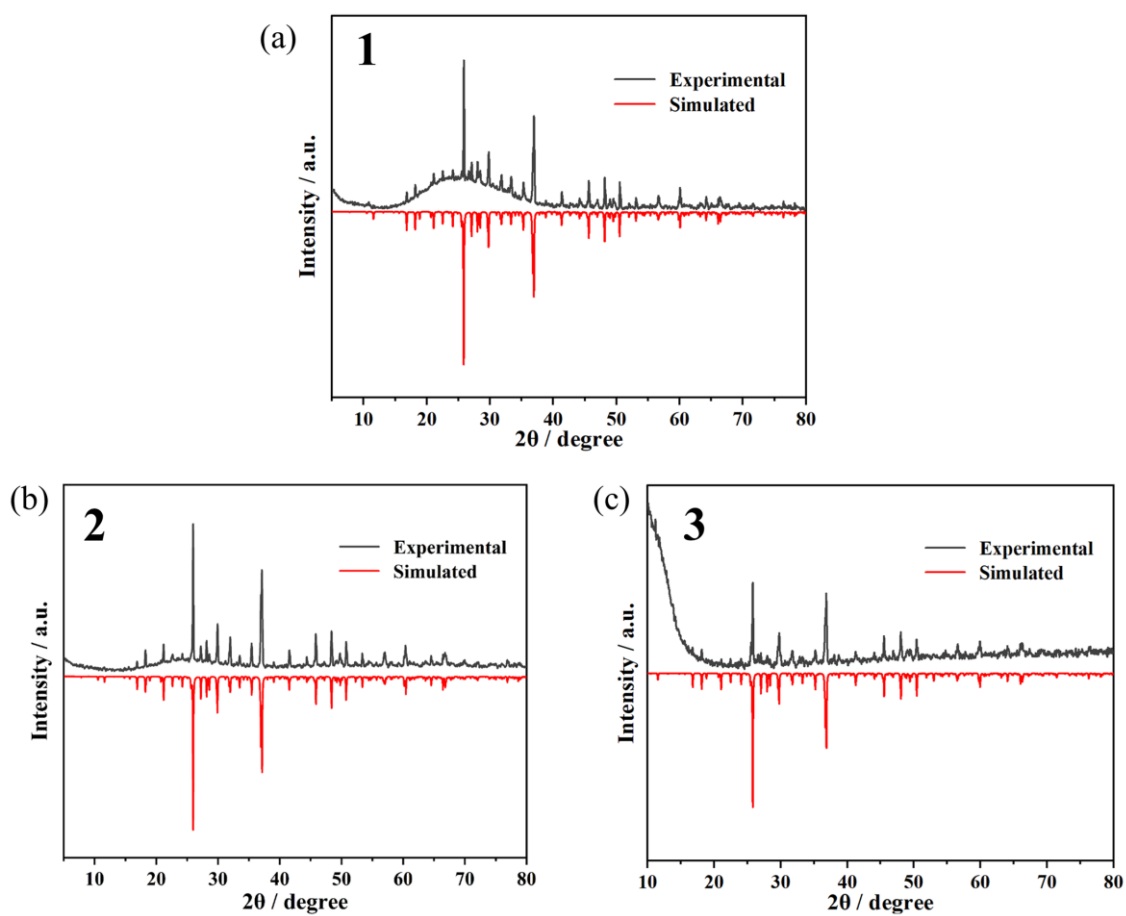


Figure S2. The powder XRD patterns of **1** (a), **2** (b) and **3** (c).

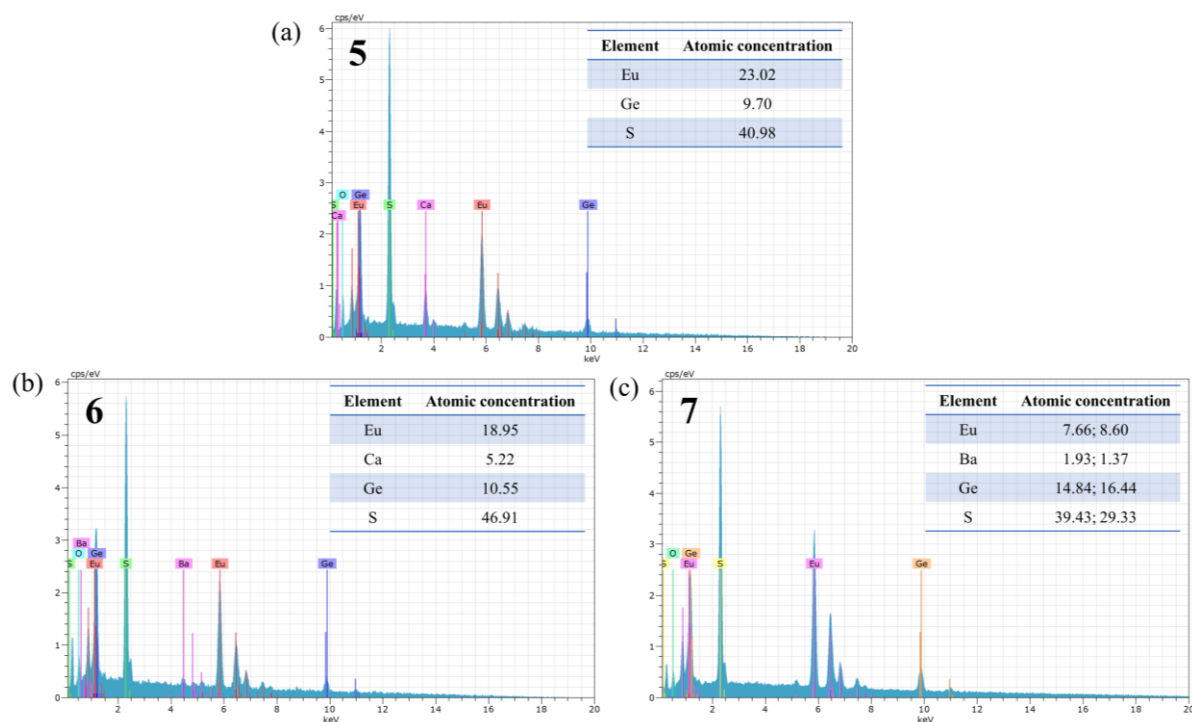


Figure S3. The EDS images for single crystals of 1 (a), 2 (b) and 3 (c).

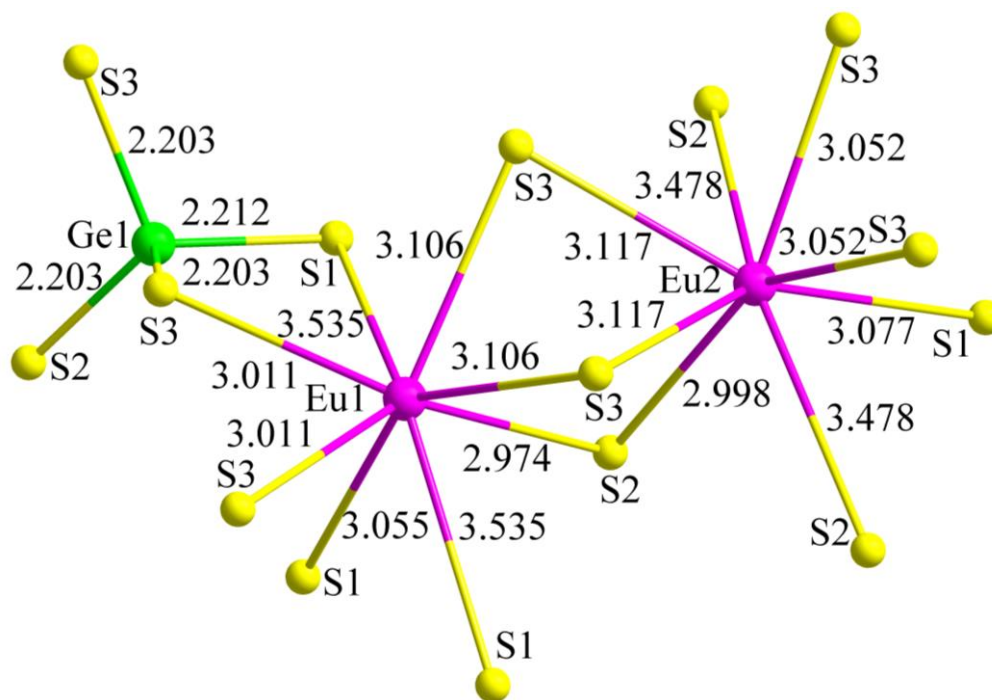


Figure S4. Coordination geometry of 0.

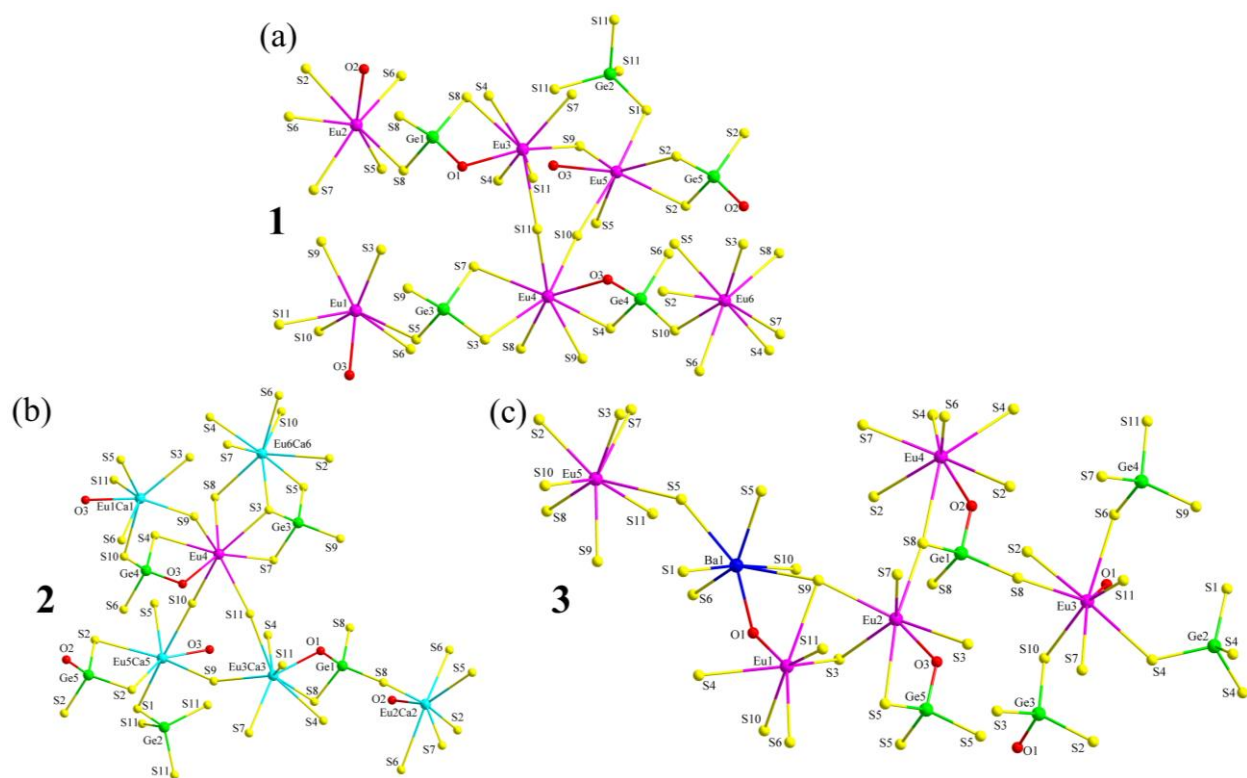


Figure S5. Coordination geometries of **1** (a), **2** (b) and **3** (c).

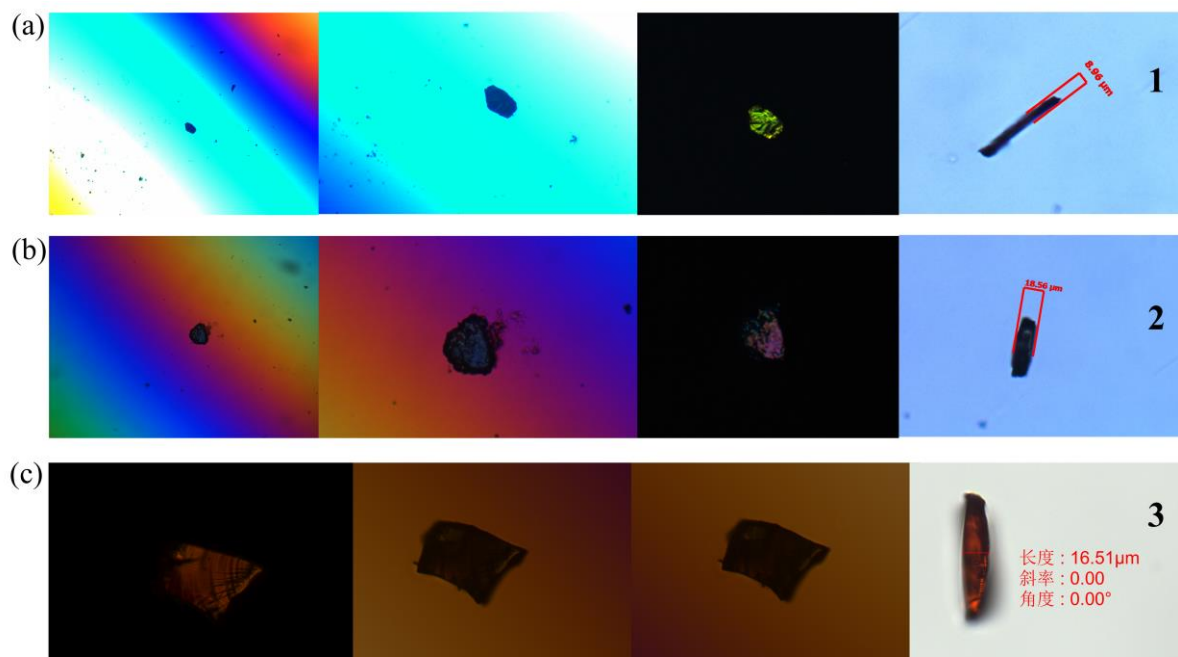


Figure S6. Photographs of **1** (a), **2** (b) and **3** (c) for the measurements of birefringence with polarizing microscope.

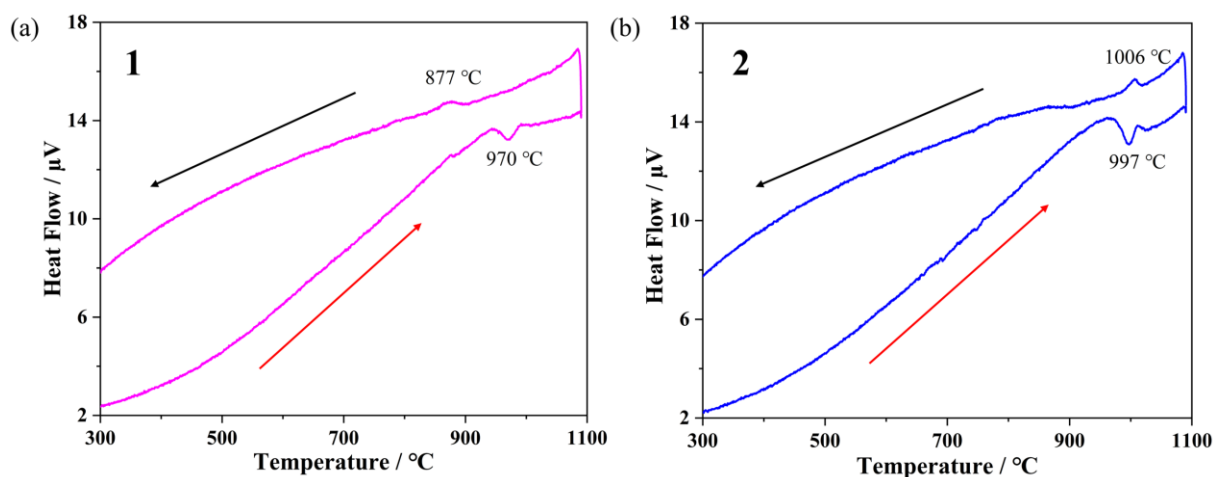


Figure S7. DSC curves of **1** and **2**. The red and black arrows represent the heating and cooling processes, respectively.

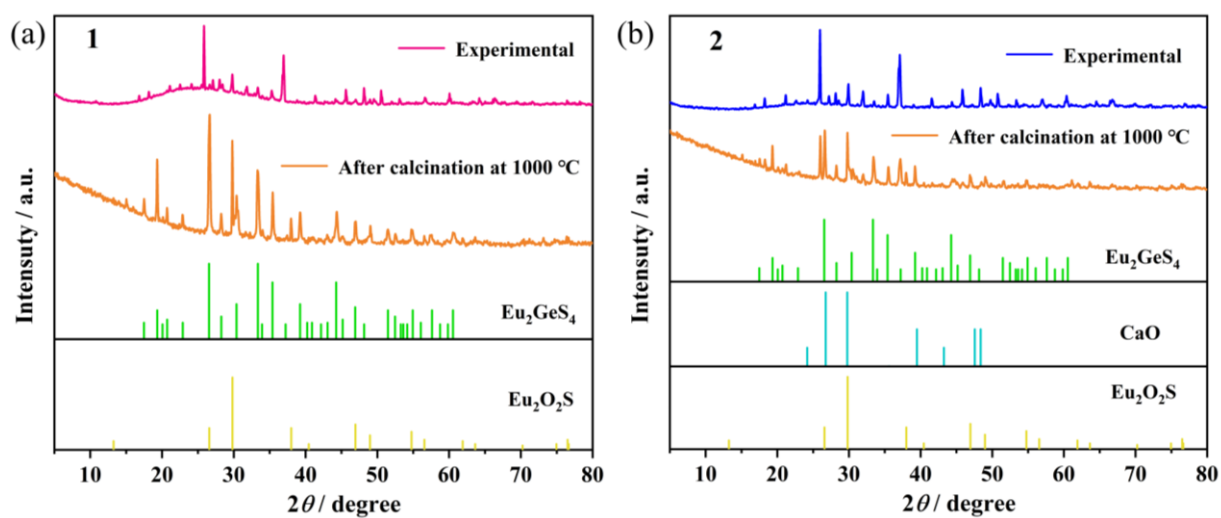


Figure S8. The powder XRD patterns of **1** and **2** after calcination.

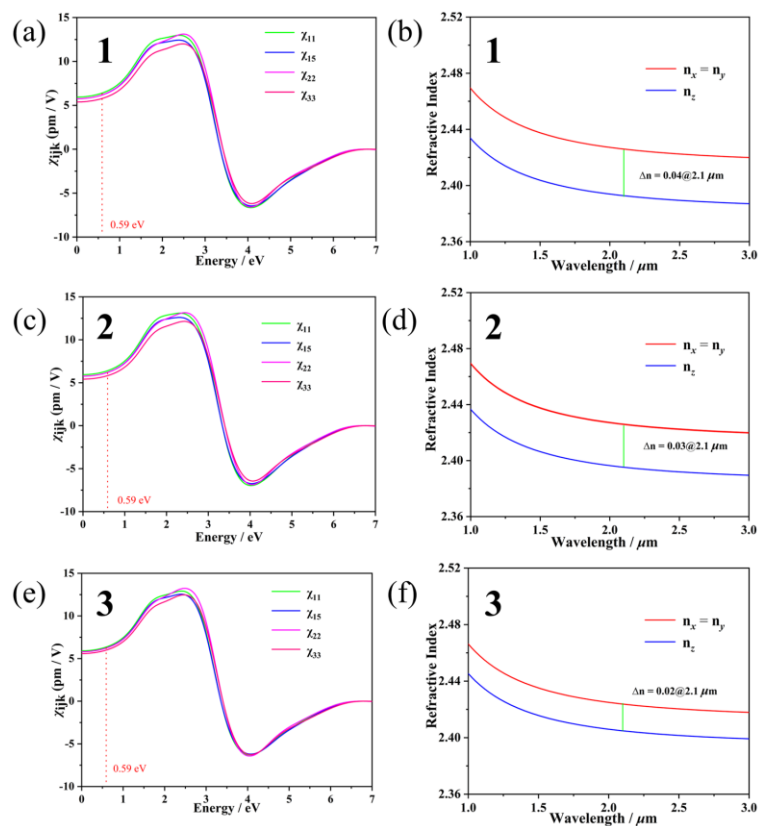


Figure S9. The calculated SHG tensors (a, c, e) and birefringences (b, d, f) of 1–3.

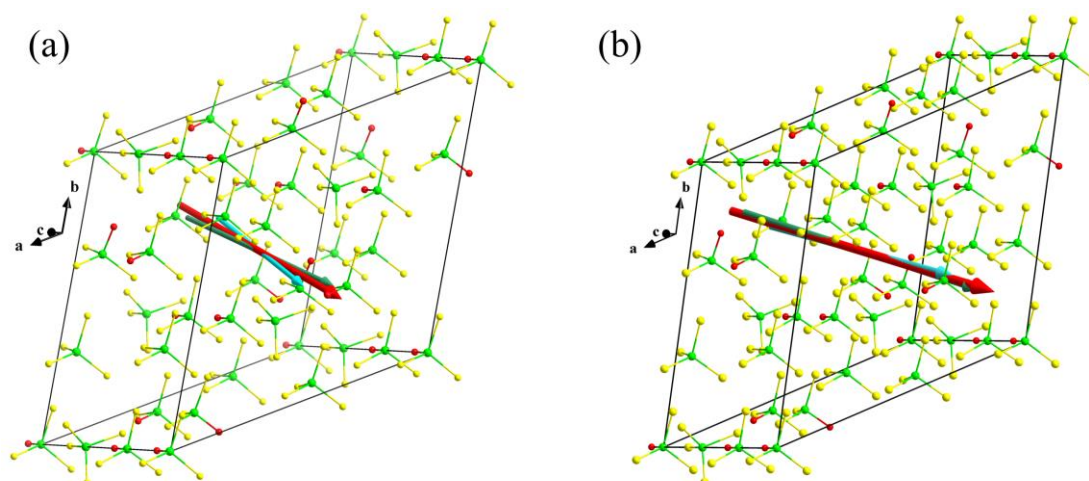


Figure S10. The calculated dipole moments for one unit cell of 1 (a) and 2 (b) (Red: total; blue: GeS₄ tetrahedra; green: GeOS₃ tetrahedra).

3. References

1. X. Lian, Z.-T. Lu, W.-D. Yao, S.-H. Yang, W. L. Liu, R.-L. Tang, S.-P. Guo, Structural Transformation and Second-Harmonic-Generation Activity in Rare-Earth and d^0 Transition-Metal Oxysulfides $RE_3NbS_3O_4$ ($RE = Ce, Sm, Gd, Dy$), *Inorg. Chem.* 2021, **60**, 10885–10889.
2. H. Yan, Y. Matsushita, K. Yamaura, Y. Tsujimoto, $La_3Ga_3Ge_2S_3O_{10}$: An Ultraviolet Nonlinear Optical Oxysulfide Designed by Anion-Directed Band Gap Engineering, *Angew. Chem. Int. Ed.* 2021, **60**, 26561–26565.
3. J. J. Xu, K. Wu, Y. Xiao, B. B. Zhang, H. H. Yu, H. J. Zhang, Mixed-Anion-Oriented Design of $LnMGe_3S_6O$ ($Ln = La, Pr, \text{ and } Nd; M = Ca \text{ and } Sr$) Nonlinear Optical Oxysulfides with Targeted Property Balance, *ACS Appl. Mater. Interfaces.* 2022, **14**, 37967–37974.
4. M. Yang, W. D. Yao, W. L. Liu, S. P. Guo, The first quaternary rare-earth oxythiogermanate with second-harmonic generation and ferromagnetic behavior, *Chem. Commun.* 2023, **59**, 3894–3897.
5. M. Y. Ran, S. H. Zhou, W. B. Wei, B. X. Li, X. T. Wu, H. Lin, Q. Li. Zhu, Rational Design of a Rare-Earth Oxychalcogenide $Nd_3[Ga_3O_3S_3][Ge_2O_7]$ with Superior Infrared Nonlinear Optical Performance, *Small.* 2023, **19**, 2300248.
6. N. Zhang, X. Huang, W. D. Yao, Y. Chen, Z. R. Pan, B. X. Li, W. L. Liu, S. P. Guo, $Eu_2MGe_2OS_6$ ($M = Mn, Fe, Co$): Three Melilite-Type Rare-Earth Oxythiogermanates Exhibiting Balanced Nonlinear-Optical Behaviors, *Inorg. Chem.* 2023, **62**, 16299–16303.